EXCESS ELECTRONS IN AMMONIA CLUSTERS

R.N. BARNETT, Uzi LANDMAN, C.L. CLEVELAND

School of Physics, Georgia Institute of Technology, Atlanta, GA 30332, USA

N.R. KESTNER

Department of Chemistry, Louisiana State University, Baton Rouge, LA 70803, USA

and

Joshua JORTNER

School of Chemistry, Tel Aviv University, 69978 Tel Aviv, Israel

Electron attachment and localization to ammonia clusters, $(NH_3)_n^-$ ($n=16$–256), is studied using path-integral molecular simulations, employing an electron–molecule pseudopotential which includes Coulomb, polarization, exclusion and exchange contributions. Due to the nature of the interactions the ammonia clusters do not form stable well-bound surface states for any size, in contrast to medium-size water clusters. The onset of bound excess electron states in ammonia clusters occurs for $n \gtrsim 32$, via an internal localization mode, in agreement with experiment.

The solvated electron in liquid ammonia was experimentally discovered in the 19th century. Sir Humphrey Davy recorded in a laboratory notebook dated November 1808 [1] the properties of blue and bronze solutions obtained by the exposure of potassium to ammonia, while Weyl published in 1864 his studies of metal–ammonia solutions [2]. The solvated electron in water is of a more recent vintage, being generated by Hart and Boag in 1962 via pulse radiolysis of water [3]. Non-reactive electron localization in these and other polar fluids [4–7] provided a theoretical challenge in the general area of electronic states of liquids, elucidating the effects of long-range [8] and short-range [9–12] attractive electron–solvent interactions and the role of local solvent reorganization on the structure, energetics, charge distribution and optical properties of the excess electron. The recent discovery [13–18] of electron attachment to finite clusters of polar molecules, e.g. $(H_2O)_n$ and $(NH_3)_n$, opens new avenues [19–24] for microscopic studies of electron solvation and localization in finite systems.

The advent of supersonic and cluster beams which allow accurate investigations [13–18] of size effects and energetics of electron attachment to well characterized systems revealed that while the onset of stability of negatively charged $(H_2O)_n^-$ clusters occurs for $n \gtrsim 11$ [13,14,16–18], negatively charged $(NH_3)_n^-$ clusters were observed only for $n \gtrsim 30$ [15]. This pronounced difference cannot be explained in terms of the variation in the molecular dipole moment (1.85 and 1.47 D for H_2O and NH_3, respectively) since the electron–molecule interaction consists of additional important contributions [21–23,25] and furthermore the mechanism and energetics of solvation involve solvent reorganization governed by intermolecular interactions beyond the dipolar interactions.

Recently [21–23] we have applied the quantum path-integral molecular-dynamics (QUPID) method to explore the localization modes of an excess electron in $(H_2O)_n^-$ clusters over a broad range of cluster sizes ($n=8$–128) and over a wide temperature domain ($T=79$–300 K), employing a newly con-

structed pseudopotential for the electron–molecule interaction [21–23] which consists of Coulomb, polarization, exclusion and exchange contributions. A major conclusion from these studies is that electron localization in medium-sized $(8 \leqslant n \leqslant 32)$ water clusters occurs via a novel *excess electron surface state on the water cluster* [21–23] and only upon increasing the size of the water clusters above $n > 32$ does the interior electron localization mode become energetically favored [23]. Furthermore, we have shown [23,26] that the calculated vertical and adiabatic (i.e. including cluster molecular reorganization) binding energies of the compact, interior excess electron states, exhibit a linear dependence on $n^{-1/3}$, in quantitative agreement with the implications of dielectric medium effects formulated for finite systems [23,26]. The calculated [21–23] vertical binding energies for the surface states of the smaller clusters $(n \leqslant 18)$ agree [22,23] with those measured [16] via photoelectron spectroscopy.

In this Letter we show, on the basis of QUPID calculations, that $(NH_3)_n^-$ clusters of all sizes do not support well bound excess electron surface states, in contrast to the $(H_2O)_n^-$ clusters. Furthermore, we conclude that as a result of the above and coupled with the competing effects of electron binding and molecular reorganization, the onset of stable well bound, interior states in $(NH_3)_n^-$ requires clusters with $n > 30$, thus explaining the experimental observations for ammonia clusters and the difference between them and the critical sizes in $(H_2O)_n^-$ clusters.

The QUPID method [*1] rests on an isomorphism between the quantum problem and a classical one, wherein the quantum particle is represented by a necklace of P pseudo particles ("beads") with nearest-neighbor harmonic interactions [20–23,25,27]. Invoking previous formalism and notation [21–23] the average total energy of the system is

$$E = 3(4n)/2\beta + \langle V_c \rangle + K + P^{-1} \sum_{i=1}^{P} \langle V(r_i) \rangle$$

with $K = 3/2\beta + K_{int}$, where V_c is the interaction potential between the classical particles, $V(r_i)$ is the cluster–electron interaction for the ith pseudoparticle,

$$K_{int} = \frac{1}{2P} \sum_{i=1}^{P} \left\langle \frac{\partial V(r_i)}{\partial r_i} \cdot (r_i - r_P) \right\rangle ,$$

[*1] For a recent review, see ref. [27]; see also refs. [20–23,25].

$\beta = 1/kT$ and $\langle \; \rangle$ indicates statistical averaging, and n is the number of ammonia molecules in the cluster. The ammonia molecules in this study were treated classically. The choice of the number of beads, P, representing the excess electron is temperature dependent. As a rule of thumb we found that an adequate discretization of the electron path is achieved for $PkT \geqslant e^2/a_0$. The integration of the equations of motion for the classically isomorphic system was performed at constant temperature (canonical ensemble) with the velocity form of the Verlet integration algorithm [21–23].

A key issue in modeling the system is the choice of interaction potentials. For the intermolecular interactions between ammonia molecules we used the potential proposed by Hinchliffe et al. [28] [*2], and for the intramolecular interactions we employed a harmonic valence-coordinate model potential based on a four-force-constant model [29] which was fitted [29] to the molecular spectroscopic data. For the electron–ammonia interaction we used the local pseudo-potential which we have constructed [21–23] in the spirit of the density functional theory, consisting of Coulomb, polarization, exclusion and exchange contributions [*3].

The energetics of the $(NH_3)_n^-$ clusters is expressed in terms of the electron vertical binding energy (EVBE), electron adiabatic binding energy (EABE) and cluster reorganization energy (E_c),

$$EVBE = K_{int} + \langle V \rangle , \tag{1}$$

$$EABE = EVBE + E_c , \tag{2}$$

$$E_c = \langle V_c \rangle_{(NH_3)_n^-} - \langle V_c \rangle_{(NH_3)_n}. \tag{3}$$

The cluster reorganization energy (eq. (3)) is the difference between the equilibrium intramolecular and intermolecular potential energies in the negatively charged $((NH_3)_n^-)$ and the corresponding neutral $((NH_3)_n)$ clusters. EVBE is the energy re-

---

[*2] We use the "Model C" intermolecular potential.

[*3] The molecular electronic charge distribution which enters the expressions for the exclusion and exchange contributions was calculated using a 6-31G** basis with the extra d orbital from ref. [30]. The coefficient $\alpha_x = 0.25$ was used in the exchange potential and $R_p = 1.7 \; a_0$ in the expression for the adiabatic polarization potential with the molecular spherical polarizability [28] $\alpha = 14.98 \; a_0^3$. For details of the pseudopotential see refs. [21–23].

quired to detach the electron from the $(NH_3)_n$ cluster without allowing nuclear rearrangement to occur and is the quantity measured in photoelectron spectroscopy [15] and EABE is the heat of solution of the excess electron in the cluster. The energetic stability of the negatively charged cluster with respect to the equilibrium neutral cluster plus free electron is inferred from the magnitude and sign of EABE, with a negative value corresponding to an energetically stable bound state.

Results pertaining to the energetics of equilibrium $(NH_3)_n^-$ clusters at $T=189.5$ K (compare to the melting point of ammonia at 195.45 K) for n in the range 16 to 256 are given in table 1 along with the corresponding radii of gyration R_g of the excess electron distribution (in all calculations $P=2048$ to ensure proper discretization of the electron path). We note first that for clusters with $n<32$ no internal states form and conversely no surface states form for $n>32$. In fact the surface states for $n=16$ and 24 develop from an attempt to form internal states for these clusters and an internal state for $n=64$ evolved from an attempt to form a surface state for this cluster. The surface states which we found for $n=24$ and 32 are relatively weakly bound (small EVBE values) in a diffuse (large R_g) state (simulations at lower temperatures did not improve the stability of these states). Furthermore, even for a medium-size cluster ($n=16$) we predict no stable excess electron bound

Table 1
Energetics of excess electron localization via internal and surface states in $(NH_3)_n$. EVBE and EABE are the electron vertical and adiabatic binding energies, respectively (eqs. (1) and (2)), and E_c is the cluster reorganization energy (eq. (3)). R_g is the radius of gyration of the electron (bead) distribution. Energies in eV and R_g in unit of Bohr radius $a_0=0.5218$ Å

n	EVBE	EABE	E_c	R_g
internal states				
<32	no internal states			
32	−1.763	−0.087	1.676	4.1
64	−2.517	−0.376	2.141	3.9
128	−2.853	−0.462	2.391	3.8
256	−3.139	−0.619	2.520	4.0
surface states				
16	−0.213	0.020	0.233	10.8
24	−0.342	−0.026	0.316	9.7
32	−0.435	−0.112	0.323	8.8
>64	no surface states			

state (EABE>0), and for $n=24$ only a marginally stable weakly bound surface state is found (EABE$=-0.026$). As is evident from table 1 the cluster molecular reorganization energies (E_c, see eq. (3)) accompanying localization in internal states are much larger than those corresponding to the weakly bound surface states.

Analysis of excess electron localization in the internal mode in which the molecular cluster is modeled by a dielectric sphere [26] yields the following expressions for the electron vertical and adiabatic binding energies,

$$EVBE(\bar{R}) = EVBE(\infty) + An^{-1/3}, \qquad (4)$$

$$EABE(\bar{R}) = EABE(\infty) + Bn^{-1/3}, \qquad (5)$$

where $EVBE(\infty)$ and $EABE(\infty)$ are identified as the photoelectric threshold and heat of solution in the bulk, $\bar{R}=r_s n^{-1/3}$, where r_s in the (mean) radius of the molecular constituent, n is the number of molecules in the cluster and B and A are constants expressed in terms of the static (D_s) and optical (D_{op}) dielectric constants,

$$B = (e^2/2r_s)(1-D_s^{-1})$$

and

$$A = (e^2/2r_s)(1+D_{op}^{-1}-2D_s^{-1}).$$

Motivated by the predicted functional dependence of the binding energies on cluster size we summarize our results for ammonia and water clusters in fig. 1. As evident from the figure the predicted linear dependence of the binding energies for internal localization on $n^{-1/3}$ is exhibited for both $(H_2O)_n^-$ and $(NH_3)_n^-$ clusters. Moreover the values of the predicted slopes (A and B) calculated by using proper values for the material parameters agree with the simulation results. From the data for the internal states we find that the predicted asymptotic values ($n\to\infty$) for EABE for water and ammonia are in agreement with the current experimental estimates [11] (-1.7 and ≈ -1.1 eV for water and ammonia, respectively) for the bulk heats of solution of an excess electron in these materials. For the $(NH_3)_n^-$ clusters we observe that the onset of stable (negative electron adiabatic binding energy, EABE) electron localization occurs for $n\gtrsim 32$ and that the electron is bound in an *internal state*. In contrast to the case of the $(H_2O)_n^-$ clusters [21–23], the internal locali-
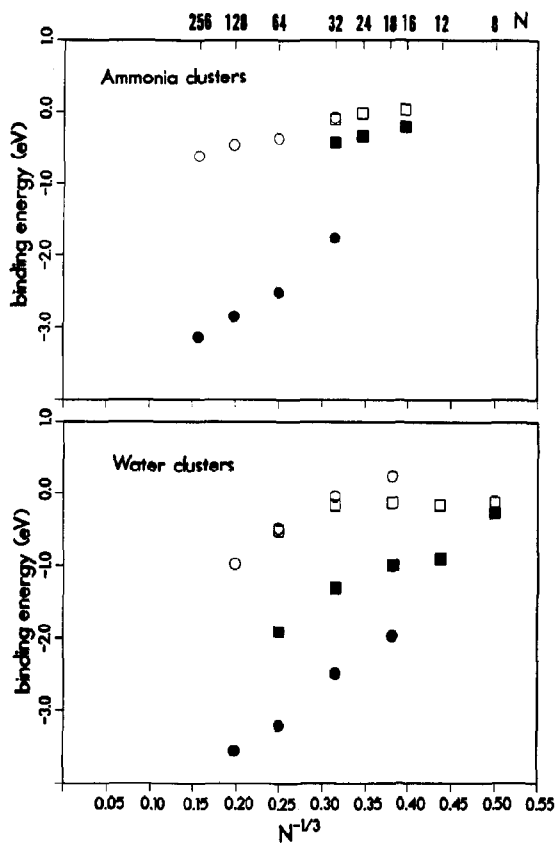
Fig. 1. Calculated excess electron energies (in eV) versus $n^{-1/3}$ for $(NH_3)_n^-$ (a) and $(H_2O)_n^-$ (b) clusters. Circles and squares correspond to interior and surface states, respectively. Full and empty symbols correspond to the vertical (EVBE) and adiabatic (EABE) binding energies respectively. The ammonia results were obtained at $T = 189.5$ K and those for water [21–23] at $T = 300$ K for $n \gtrsim 32$ and $T = 79$ K for $n < 32$. Note the weaker binding in ammonia relative to water, in particular for the surface states, and the linear dependence on $n^{-1/3}$ for the internal states.

zation in ammonia clusters with $n \gtrsim 32$ is not preceded by a stable well-bound surface state for smaller cluster sizes. Thus the energetic instability of the surface states on ammonia clusters which originates from the nature of the electron–molecule interaction and the intermolecular interactions is identified as the reason for the observed different minimal sizes of clusters of these two polar materials ($n \gtrsim 11$ for water [13,14,16–18] and $n \gtrsim 30$ for ammonia [15]) which sustain bound states of an excess electron.

[1] P.P. Edwards, Advan. Inorg. Radiochem. 25 (1982) 135.

[2] W. Weyl, Ann. Phys. 197 (1863) 601.

[3] E.J. Hart and J.W. Boag, J. Am. Chem. Soc. 84 (1962) 4090.

[4] G. Lepoutre and M. Sienko, eds., Solutions metal–ammonia (Benjamin, New York, 1964).

[5] J.J. Lagowski and M. Sienko, eds., Metal–ammonia solutions (Butterworths, London, 1970).

[6] J. Jortner and N.R. Kestner, eds., Electrons in fluids (Springer, Berlin, 1973).

[7] Can. J. Chem. 55 (1977) 1795–2277.

[8] J. Jortner, J. Chem. Phys. 30 (1959) 839.

[9] D.A. Copeland, N.R. Kestner and J. Jortner, J. Chem. Phys. 53 (1970) 1189.

[10] J. Jortner, Ber. Bunsenges. Physik. Chem. 75 (1971) 646.

[11] M. Newton, J. Chem. Phys. 58 (1973) 5833.

[12] M. Newton, J. Phys. Chem. 79 (1975) 2795.

[13] H. Haberland, H. Langosch, H.G. Schindler and D.R. Worsnop, Surface Sci. 156 (1985) 157.

[14] H. Haberland, H.G. Schindler and D.R. Worsnop, J. Chem. Phys. 81 (1984) 3742.

[15] H. Haberland, H.G. Schindler and D.R. Worsnop, Ber. Bunsenges. Physik. Chem. 88 (1984) 270.

[16] J.V. Coe, D.R. Worsnop and K.H. Bowen, J. Chem. Phys., to be published.

[17] M. Knapp, O. Echt, D. Kreisle and E. Recknagel, J. Chem. Phys. 85 (1986) 636.

[18] M. Knap, O. Echt, D. Kreisle and E. Recknagel, J. Phys. Chem. 91 (1987) 2601.

[19] B.R. Rao and N.R. Kestner, J. Chem. Phys. 80 (1984) 1587.

[20] A. Wallqvist, D. Thiramalai and B.J. Berne, J. Chem. Phys. 85 (1986) 1583.

[21] U. Landman, R.N. Barnett, C.L. Cleveland and J. Jortner, J. Phys. Chem. 91 (1987) 4890.

[22] R.N. Barnett, U. Landman, C.L. Cleveland and J. Jortner, Phys. Rev. Letters 59 (1987) 811.

[23] R.N. Barnett, U. Landman, C.L. Cleveland and J. Jortner, J. Chem. Phys. 1988), to be published.

[24] P. Stampfli and K.H. Bennemann, Phys. Rev. Letters 58 (1987) 2635.

[25] J. Schnitker and P.J. Rossky, J. Chem. Phys. 86 (1987) 3462.

[26] R.N. Barnett, U. Landman, C.L. Cleveland and J. Jortner, Chem. Phys. Letters 145 (1988) 382.

[27] B.J. Berne and D. Thirumalai, Ann. Rev. Phys. Chem. 37 (1986) 401.

[28] A. Hinchliffe, D.G. Bounds, M.L. Klein, I.R. McDonald and R. Righini, J. Chem. Phys. 74 (1981) 1211.

[29] G. Herzberg, Infrared and Raman spectra (Van Nostrand Reinhold, New York, 1945) table 43, p. 177.

[30] Z. Latajka and S. Scheiner, J. Chem. Phys. 84 (1986) 341.